2017 American Control Conference
Sheraton Seattle Hotel
May 24–26, 2017, Seattle, USA

Closed-Form Controlled Invariant Sets for Pedestrian Avoidance

Yasser Shoukry, Paulo Tabuada, Stephanie Tsuei, Mark B. Milam, Jessy W. Grizzle, and Aaron D. Ames

***Abstract*— The recent trends in the automotive industry towards autonomous vehicles bring the problem of pedestrian avoidance to the forefront of a long list of safety concerns. In this paper we propose a closed-form solution to this problem by explicitly computing closed-form expressions for subsets of the state space where an autonomous vehicle is guaranteed to avoid collisions with a pedestrian. These sets, being controlled invariant, immediately lead to control laws for pedestrian avoidance.**

I. Introduction

In this paper we discuss a particular type of collision avoidance problem involving an autonomous vehicle and a pedestrian. Our motivation stems from the recent interest in autonomous and semi-autonomous vehicles that are expected to populate our roads in the future. One important advantage of autonomous and semi-autonomous vehicles is the potential for avoiding collisions due to distracted driving. However, avoiding collisions with pedestrians is especially challenging since pedestrians are difficult to detect through existing sensors while their intentions and behavior are often difficult to predict.

Several different collision avoidance problems have been investigated in the literature. Closer to the methods described in this paper are those papers that model collision avoidance as a game between a pursuer and an evader. In particular, the homicidal chauffeur game, in which the chauffeur tries to run over a pedestrian, is a particularly good description of our problem provided that we reverse the roles of the chauffeur and the pedestrian. Devising a strategy to avoid a collision with a pedestrian requires us to treat the pedestrian as the (homicidal!) pursuer while treating the (autonomous) chauffeur as the evader. This game has also been called the suicidal pedestrian differential game in [1]. A wealth of knowledge is available on the solution of the homicidal chauffeur game. Isaacs' book [2] provides a very readable account of the results known in the sixties whereas a survey of recent results can be found in [3].

This work was partially supported by the NSF CPS Frontiers project 1239085.

Yasser Shoukry is with both the UC Berkeley Electrical Engineering and Computer Science Department, Berkeley, CA and the UCLA Electrical Engineering Department, Los Angeles, CA, yshoukry@eecs.berkeley.edu

Paulo Tabuada is with the UCLA Electrical Engineering Department, Los Angeles, CA, tabuada@ee.ucla.edu

Stephanie Tsuei and Mark B. Milam are with NG Next, Northrop Grumman, Redondo Beach, CA, {Stephanie.Tsuei, Mark.Milam}@ngc.com

Jessy W. Grizzle is with the Department of Electrical Engineering and Computer Science, University of Michigan, Ann Arbor, MI, USA., grizzle@umich.edu

Aaron D. Ames is with the Department of Mechanical and Civil Engineering, California Institute of Technology, Pasadena, CA, ames@caltech.edu

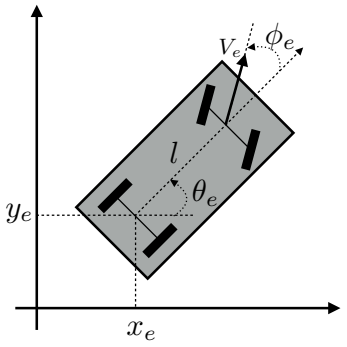

Fig. 1. Graphical description of the state variables used to mode the autonomous vehicle (evader).

Despite a considerable amount of research on pursuit evasion games it is not always possible to obtain a closed-form solution that characterizes the escaping strategy for the evader. For this reason, several computational approaches have been investigated in the literature such as sampling based methods [4] or reach-set techniques [5]. The contribution of this paper is to show that through very elementary arguments we can compute closed-form expressions for controlled-invariant sets that exclude collisions. Compared to the previously mentioned computational approaches, the simpler solution described in this paper has a smaller computational cost but is only applicable to the specific collision avoidance problem in this paper.

References [1], [6], [7] provide complete solutions for the pedestrian avoidance problem for the simpler case when the vehicle is modeled as a unicycle. In this paper, we consider the more realistic front-wheel drive kinematics and construct a closed-form expression for a controlled invariant set that excludes collisions. Since the set is controlled invariant, it is possible to remain in the set forever thereby forever avoiding collisions. Moreover, controlled invariant sets naturally define feedback control laws for collision avoidance. It suffices to pick a control input that forces the evading autonomous vehicle to remain in the invariant set. For this reason, we focus on the problem of computing controlled invariant sets rather than deriving control laws although we return to this issue in the conclusions section.

II. Models

We model the pedestrian avoidance problem as a pursuit-evasion game where the pedestrian plays the role of the pursuer and the autonomous vehicle plays the role of the

evader. The autonomous vehicle (evader) is a front-wheel drive car whose kinematics is given by [8]:

$$\dot{x}_e = V_e \cos\theta_e \cos\phi_e \quad (1)$$
$$\dot{y}_e = V_e \sin\theta_e \cos\phi_e \quad (2)$$
$$\dot{\theta}_e = \frac{V_e}{l} \sin\phi_e \quad (3)$$
$$\dot{\phi}_e = \texttt{SAT}(\omega_e, \underline{\phi}_e, \overline{\phi}_e), \quad (4)$$

where $(x_e, y_e) \in \mathbb{R}^2$ denotes the position of the rear axle's center, V_e denotes the velocity of the front (driving) wheel, $\theta_e \in \mathbb{S}$ denotes its orientation, l denotes the distance between the front and rear wheels, and $\phi_e \in \mathbb{S}$ denotes the front wheel orientation which is assumed to satisfy the following bounds:

$$-\pi/2 < \underline{\phi}_e \leq \phi_e \leq \overline{\phi}_e < \pi/2.$$

All these quantities are illustrated in Figure 1. The translational velocity, assumed to be constant, is denoted by $V_e \in \mathbb{R}$ while the angular velocity of the steering wheel, treated as the control input, is denoted by $\omega_e \in [\underline{\omega}_e, \overline{\omega}_e] \subseteq \mathbb{R}$. We assume that $0 \in [\underline{\omega}_e, \overline{\omega}_e]$, i.e., $\underline{\omega}_e < 0$ and $\overline{\omega}_e > 0$. Finally, the saturation function SAT is defined as:

$$\texttt{SAT}(\omega_e, \underline{\phi}_e, \overline{\phi}_e) = \begin{cases} 0 & \text{if} \quad \phi_e = \overline{\phi}_e \wedge \omega_e \geq 0 \\ 0 & \text{if} \quad \phi_e = \underline{\phi}_e \wedge \omega_e \leq 0 \\ \omega_e & \text{otherwise.} \end{cases}$$

The pedestrian (pursuer) is modeled by:

$$\dot{x}_p = u_{px} \quad (5)$$
$$\dot{y}_p = u_{py} \quad (6)$$
$$\|(u_{px}, u_{py})\| \leq V_p, \quad (7)$$

where $(x_p, y_p) \in \mathbb{R}^2$ denotes the pedestrian's position and $(u_{px}, u_{py}) \in \mathbb{R}^2$ are control inputs. Intuitively, the pedestrian can move in any direction but its maximum velocity is bounded by V_p. Note that:

$$V_p \leq V_e \quad (8)$$

is a necessary condition for collision avoidance [1]. Hence, we assume that such inequality holds throughout the paper.

In order to simplify the equations of motion, we follow three steps, namely: (i) constructing the error dynamics, (ii) aligning the error dynamics, and (iii) transforming the aligned error dynamics into polar coordinates. The details of these steps are provided below.

Step 1: Constructing the Error Dynamics

It is convenient to simplify the equations of motion by first considering the error:

$$e_x = x_e - x_p, \quad e_y = y_e - y_p$$

and obtaining the error dynamics:

$$\dot{e}_x = V_e \cos\theta_e \cos\phi_e - u_{px}$$
$$\dot{e}_y = V_e \sin\theta_e \cos\phi_e - u_{py}$$
$$\dot{\theta}_e = \frac{V_e}{l} \sin\phi_e$$
$$\dot{\phi}_e = \texttt{SAT}(\omega_e, \underline{\phi}_e, \overline{\phi}_e)$$

Step 2: Aligning the Error Dynamics

Next, we perform a clockwise rotation of θ_e radians so as to align the velocity V_e with the e_{z_1} axis. The error dynamics in the new coordinates:

$$\begin{bmatrix} e_{z_1} \\ e_{z_2} \\ \theta_e \\ \phi_e \end{bmatrix} = \begin{bmatrix} \cos\theta_e & \sin\theta_e & 0 & 0 \\ -\sin\theta_e & \cos\theta_e & 0 & 0 \\ 0 & 0 & 1 & 0 \\ 0 & 0 & 0 & 1 \end{bmatrix} \begin{bmatrix} e_x \\ e_y \\ \theta_e \\ \phi_e \end{bmatrix}$$

is given by:

$$\begin{aligned} \dot{e}_{z_1} &= -e_x\dot{\theta}_e \sin\theta_e + \dot{e}_x \cos\theta_e + e_y\dot{\theta}_e \cos\theta_e + \dot{e}_y \sin\theta_e \\ &= \frac{V_e}{l} \sin\phi_e \; e_{z_2} + V_e \cos\phi_e - v_{p1} \quad (9) \\ \dot{e}_{z_2} &= -e_x\dot{\theta}_e \cos\theta_e - \dot{e}_x \sin\theta_e - e_y\dot{\theta}_e \sin\theta_e + \dot{e}_y \cos\theta_e \\ &= -\frac{V_e}{l} \sin\phi_e \; e_{z_1} - v_{p2} \quad (10) \\ \dot{\theta}_e &= \frac{V_e}{l} \sin\phi_e \quad (11) \\ \dot{\phi}_e &= \texttt{SAT}(\omega_e, \underline{\phi}_e, \overline{\phi}_e) \quad (12) \end{aligned}$$

where:

$$v_{p1} = u_{px} \cos\theta_e + u_{py} \sin\theta_e,$$
$$v_{p2} = -u_{px} \sin\theta_e + u_{py} \cos\theta_e$$

are the pursuer's control inputs (velocity). Note that $\|(v_{p1}, v_{p2})\| = \|(u_{px}, u_{py})\| \leq V_p$. Note also that the first two equations do not depend on θ_e. Hence, we will work with the first, second and fourth equations and will drop the third equation.

Step 3: Transformation into Polar Coordinates

The final step is to transform the aligned error dynamics e_{z_1}, e_{z_2} into polar coordinates e_r, e_δ. Such transformation $(e_{z_1}, e_{z_2}) \mapsto (e_r, e_\delta)$ is defined as:

$$\begin{bmatrix} e_r \\ e_\delta \end{bmatrix} = \begin{bmatrix} \sqrt{e_{z_1}^2 + e_{z_2}^2} \\ \tan^{-1} \frac{e_{z_2}}{e_{z_1}} \end{bmatrix} \quad (13)$$

and its inverse transformation $(e_r, e_\delta) \mapsto (e_{z_1}, e_{z_2})$ is:

$$\begin{bmatrix} e_{z_1} \\ e_{z_2} \end{bmatrix} = \begin{bmatrix} e_r \cos e_\delta \\ e_r \sin e_\delta \end{bmatrix}. \quad (14)$$

Simple computations lead to the following differential equation governing the evolution of e_r is given by:

$$\dot{e}_r = V_e \cos\phi_e \cos e_\delta - (v_{p1} \cos e_\delta + v_{p2} \sin e_\delta). \quad (15)$$

Since the pursuer seeks to force a collision, its optimal strategy is the one that minimizes the distance between the pursuer and the evader e_r under the constraint $\|(v_{p1}, v_{p2})\| \leq V_p$. By inspecting (15) we note that the pursuer has control only over the second term, i.e., $v_{p1} \cos e_\delta + v_{p2} \sin e_\delta$. It is then not difficult to see that the optimal pursuer strategy is to decrease the radius by a rate equal to the maximum allowed rate which is equal to V_p, i.e., by setting:

$$v_{p1} \cos e_\delta + v_{p2} \sin e_\delta = V_p.$$

Combining the previous equality with the constraint $\|(v_{p1}, v_{p2})\| \leq V_p$, we conclude that the optimal pursuer strategy can be written as:

$$v_{p1} = V_p \cos e_\delta, \qquad v_{p2} = V_p \sin e_\delta. \tag{16}$$

By substituting in (15), we can write the error dynamics in polar coordinates as:

$$\dot{e}_r = V_e \cos\phi_e \cos e_\delta - V_p. \tag{17}$$

Similarly, the dynamics of e_δ can be obtained as:

$$\begin{aligned}
\dot{e}_\delta &= \frac{1}{1+\left(\frac{e_{z_2}}{e_{z_1}}\right)^2} \frac{d}{dt}\left(\frac{e_{z_2}}{e_{z_1}}\right) \\
&= \frac{1}{e_r^2}\left(e_{z_1}\dot{e}_{z_2} - e_{z_2}\dot{e}_{z_1}\right) \\
&= \frac{-V_e}{l}\sin\phi_e\left(\cos^2 e_\delta + \sin^2 e_\delta\right) - \frac{1}{e_r}V_e \sin e_\delta \cos\phi_e \\
&- \frac{1}{e_r}\left(\cos e_\delta v_{p2} - \sin e_\delta v_{p1}\right) \\
&= \frac{-V_e}{l}\sin\phi_e - \frac{1}{e_r}V_e \sin e_\delta \cos\phi_e
\end{aligned} \tag{18}$$

where the last equality follows from substituting the optimal strategy (16) which results in the identities:

$$\cos e_\delta v_{p2} - \sin e_\delta v_{p1} = V_p \cos e_\delta \sin e_\delta - V_p \cos e_\delta \sin e_\delta = 0.$$

III. A CONTROLLED INVARIANT SUBSET

A. A simple controlled invariant set

We start by identifying a simple controlled invariant set that will be enlarged in Section III-B.

***Proposition** 3.1:* The set:

$$\begin{aligned}
S = \big\{(e_r, e_\delta, \theta_e, \phi_e) \in \mathbb{R}\times\mathbb{S}^3 \mid \\
e_r > 0,\ e_\delta \in]-\pi/2, \pi/2[,\ \phi_e = 0\big\}.
\end{aligned}$$

is controlled invariant[1].

Proof: To show that S is controlled invariant, we start by examining the error dynamics in the (e_{z_1}, e_{z_2}) coordinates. First note that by setting the input ω_e to zero we obtain:

$$\phi_e(0) = 0 \wedge \dot{\phi}_e = 0 \Rightarrow \phi_e(t) = 0 \Rightarrow \dot{e}_{z_1} = V_e - v_{p1}$$

and the constraint $|v_{p1}| \leq \|(v_{p1}, v_{p2})\| \leq V_p \leq V_e$ (see the discussion preceding inequality (8)) implies $\dot{e}_{z_1} \geq 0$. Hence, if e_{z_1} is positive, it will remain positive since its derivative is non-negative. Now recall the definition of $e_r = \|(e_{z_1}, e_{z_2})\|_2$ from which we conclude that the following holds for all time t:

$$e_r(t) = \|(e_{z_1}(t), e_{z_2}(t))\|_2 \overset{(a)}{\geq} \|e_{z_1}(t)\|_2 \overset{(b)}{\geq} \|e_{z_1}(0)\|_2 \overset{(c)}{>} 0$$

where (a) follows from the inverse triangular inequality; (b) follows from the fact that $\dot{e}_{z_1}$ is nonnegative; and (c) follows from the constraints $e_\delta \in]-\pi/2, \pi/2[$ which implies that $e_{z_1}(0)$ satisfies $e_{z_1}(0) > 0$.

■

[1]A set S is controlled invariant if $(e_r(0), e_\delta(0), \theta_e(0), \phi_e(0)) \in S$ implies the existence of a control strategy for the evader leading to $(e_r(t), e_\delta(t), \theta_e(t), \phi_e(t)) \in S$ for all $t \geq 0$ and for every control strategy of the pursuer.

B. Enlarging the simple controlled invariant set through a collision avoidance maneuver.

We now ask the question, if $(e_r, e_\delta, \theta_e, \phi_e) \notin S$, is there a maneuver that brings the state to S while avoiding a collision? In this section, we assume without loss of generality that the pursuer starts at the origin, i.e., $x_p(0) = y_p(0) = 0$. Indeed, if the pursuer is not located at the origin at time $t = 0$, then one can always perform an affine change of coordinates to place the pursuer at the origin. Such affine change of coordinates will not affect the model derived in the previous section.

Consider the case when $e_\delta(0)$ lies in the second quadrant, i.e., $\pi/2 \leq e_\delta(0) \leq \pi$, and in order to avoid a collision, we need to decrease the angle e_δ until e_δ becomes $e_\delta(t_f) = \pi/2 - \varepsilon$, for some small enough $\varepsilon \in \mathbb{R}^+$ (recall that the definition of S does not include $e_\delta(t_f) = \pi/2$), at some time t_f. At this point t_f, and in order to enter the controlled invariant set, we need to ensure that the steering angle $\phi_e(t_f)$ is also equal to zero. Note that the dynamics of the steering angle ϕ_e suffers from a saturation behavior. Therefore, in order to decrease e_δ while achieving $\phi_e(t_f) = 0$, we consider a simple maneuver that consists of the following four steps:

(i) Increase the wheel angle ϕ_e by setting the input ω_e to its maximal value $\omega_e = \overline{\omega}$ until ϕ_e reaches its maximum limit $\overline{\phi}_e$ at time t_1.
(ii) Sustain the wheel angle at its maximum value for some time $t_2 - t_1$ by setting the input ω_e to zero until the angle e_δ reaches some critical value $e_{\delta,cr}$.
(iii) Decrease the steering wheel angle ϕ_e by setting the input ω_e to its minimal value $\omega_e = \underline{\omega}$ until ϕ_e becomes zero at time t_f.
(iv) Sustain the wheel alignment at $\phi_e(t_f) = 0$ by setting the input $\omega_e = 0$.

To summarize, we consider the following maneuver:

$$\omega_e = \begin{cases}
\overline{\omega} & \phi_e \leq \overline{\phi}_e, & (t < t_1) \\
0 & \phi_e = \overline{\phi}_e \wedge e_\delta < e_{\delta,cr}, & (t_1 \leq t < t_2) \\
\underline{\omega} & \phi_e \geq 0 & (t_2 \leq t < t_f) \\
0 & e_\delta = 0 \wedge \phi_e = 0 & t = t_f
\end{cases} \tag{19}$$

The reverse sequence is also considered whenever the angle $e_\delta(0)$ lies in the third quadrant, i.e., $-\pi/2 \leq e_\delta(0) \leq -\pi$. Similar maneuvers also can be carried for the first and fourth quadrant when the steering angle is not equal to zero. Note that this maneuver is parametrized by the value of $t_1, e_{\delta,cr}, t_2$ and t_f. In what follows, we start by analyzing the error dynamics in order to calculate the value of $e_{\delta,cr}$. Once calculated, the time instants t_1, t_2 and t_f can be characterized based on the initial conditions of the evader $(e_r(0), e_\delta(0), \phi_e(0))$, or equivalently $(x_e(0), y_e(0), \theta_e(0), \phi_e(0))$.

IV. Maneuver Characterization

In order to calculate the exact value of $e_{\delta,cr}$ and hence the values of the time instants t_1, t_2 and t_f, we need to solve several differential equations to obtain closed-form solutions. Since these equations are highly nonlinear, we will work instead with an abstraction that provides the guarantee that any controlled invariant set for the abstraction is also a controlled invariant set for the original dynamics. The abstraction is given by:

$$\dot{\widehat{e}}_r = V_e \cos\widehat{\phi}_e \cos\widehat{e}_\delta - V_p, \qquad \hat{e}_r(0) = e_r(0) = e_{r0}, \quad (20)$$

$$\dot{\widehat{e}}_\delta = \frac{-V_e}{l}\sin\widehat{\phi}_e, \qquad \widehat{e}_\delta(0) = e_\delta(0) = e_{\delta 0} \quad (21)$$

$$\dot{\widehat{\phi}}_e = \mathtt{SAT}(\omega_e, \underline{\phi}_e, \overline{\phi}_e), \qquad \widehat{\phi}_e(0) = \phi_e(0) = \phi_{e0} \quad (22)$$

where we used the $\widehat{e}_r, \widehat{e}_\delta$ to denote the abstracted state variables. Note that the only difference between the abstracted dynamics (21) and the original dynamics (18) is the absence of the second term in the $\widehat{e}_\delta$ dynamics. As we will show later, this term helps the evader to escape faster. Thus, by eliminating this term, our solution will be more conservative (smaller controlled invariant set), however removing this term leads to a simpler nonlinear dynamics that can be solved in closed-form. In what follows, we analyze the proposed evading strategy for the abstracted dynamics.

A. Characterizing the Value of $\widehat{e}_{\delta,cr}$:

Recall that the controlled invariant set S asks for both the constraints $\widehat{\phi}_e = 0$ and $\widehat{e}_\delta = \pi/2 - \varepsilon$ to be achieved simultaneously. Therefore, while decreasing the value of e_δ, there exists a critical value $\widehat{e}_{\delta,cr}$ at which the steering wheel angle $\widehat{\phi}_e$ must be decreased (by setting $\omega_e = \underline{\omega}$) so that both $\widehat{e}_\delta$ and $\widehat{\phi}_e$ become $\widehat{e}_\delta = \pi/2 - \varepsilon, \widehat{\phi}_e = 0$ at the same time instant. In this subsection, we calculate the value of $\widehat{e}_{\delta,cr}$.

In order to calculate the value of $\widehat{e}_{\delta,cr}$, we need to consider the dynamics of the last phase. In the last phase, and starting from $\widehat{\phi}_e(t_2) = \overline{\phi}_e$ and $\widehat{e}_\delta(t_2) = \widehat{e}_{\delta,cr}$, we set $\omega_e = \underline{\omega}$ for time $\widehat{t}_2 \le t < \widehat{t}_f$. Therefore, in this time period, we have:

$$\dot{\widehat{\phi}}_e = \underline{\omega} \Rightarrow \widehat{\phi}_e(t) = \underline{\omega}(t - \widehat{t}_2) + \overline{\phi}_e.$$

This phase will take an amount of time $\widehat{t}_f - \widehat{t}_2$ obtained as follows:

$$\widehat{\phi}(t_f) = 0 \Rightarrow 0 = \underline{\omega}(\widehat{t}_f - \widehat{t}_2) + \overline{\phi}_e \Rightarrow (\widehat{t}_f - \widehat{t}_2) = \frac{-\overline{\phi}_e}{\underline{\omega}}. \quad (23)$$

Recall that $\underline{\omega}$ is negative and so the term $(\widehat{t}_f - \widehat{t}_2)$ is positive. Within this time period, the angle $\widehat{e}_\delta(t)$ decreases as:

$$\dot{\widehat{e}}_\delta = \frac{-V_e}{l}\sin\left(\underline{\omega}(t - \widehat{t}_2) + \overline{\phi}_e\right) \Rightarrow$$
$$\widehat{e}_\delta(t) = \frac{V_e}{l\underline{\omega}}\cos\left(\underline{\omega}(t - \widehat{t}_2) + \overline{\phi}_e\right) + \left(\widehat{e}_{\delta,cr} - \frac{V_e}{l\underline{\omega}}\cos\overline{\phi}_e\right).$$

This phase should end when $\widehat{e}_\delta(\widehat{t}_f) = \pi/2 - \varepsilon$. We can use this fact in order to determine the critical value $e_{\delta,cr}$ at which the third phase starts:

$$\widehat{e}_{\delta,cr} = \left(\frac{\pi}{2} - \varepsilon\right) + \frac{V_e}{l\underline{\omega}}\Big(\cos\overline{\phi}_e - \cos\left(\underline{\omega}\left(\widehat{t}_f - \widehat{t}_2\right) + \overline{\phi}_e\right)\Big)$$
$$= \left(\frac{\pi}{2} - \varepsilon\right) + \frac{V_e}{l\underline{\omega}}\cos\overline{\phi}_e \quad (24)$$

where the second equality follows from (23).

B. Characterizing the Value of $\widehat{t}_1$:

Recall that the time instant $\widehat{t}_1$ signals the end of the first phase in which we increase the steering angle $\widehat{\phi}_e$ from its initial position $\widehat{\phi}_e(0) = \phi_{e0}$ to the maximum value $\widehat{\phi}_e(\widehat{t}_1) = \overline{\phi}_e$. Within this time period $0 \le t < \widehat{t}_1$, we have:

$$\dot{\widehat{\phi}}_e = \overline{\omega} \Rightarrow \widehat{\phi}_e(t) = \overline{\omega}t + \phi_{e0}.$$

We end this phase whenever the angle $\widehat{\phi}_e(\widehat{t}_1)$ reaches its maximum, that is:

$$\widehat{\phi}_e(\widehat{t}_1) = \overline{\phi}_e \Rightarrow \overline{\phi}_e = \overline{\omega}\widehat{t}_1 + \phi_{e0} \Rightarrow \widehat{t}_1 = \frac{\overline{\phi}_e - \phi_{e0}}{\overline{\omega}}. \quad (25)$$

Within this time period, the angle $\widehat{e}_\delta$ decreases as follows:

$$\dot{\widehat{e}}_\delta = \frac{-V_e}{l}\sin\left(\overline{\omega}t + \phi_{e0}\right) \Rightarrow$$
$$\widehat{e}_\delta(t) = \frac{V_e}{l\overline{\omega}}\cos\left(\overline{\omega}t + \phi_{e0}\right) + \left(e_{\delta 0} - \frac{V_e}{l\overline{\omega}}\cos\phi_{e0}\right)$$
$$= e_{\delta 0} - \frac{V_e}{l\overline{\omega}}(\cos\phi_{e0} - \cos\left(\overline{\omega}t + \phi_{e0}\right)). \quad (26)$$

C. Characterizing the Value of $\widehat{t}_2$:

Recall that the time instant $\widehat{t}_2$ signals the end of the second phase, during which the steering angle was sustained at its maximum value $\phi_e(t) = \overline{\phi}_e$ for $\widehat{t}_1 \le t < \widehat{t}_2$. During this time period, the angle $\widehat{e}_\delta$ decreases by:

$$\dot{\widehat{e}}_\delta = \underbrace{\frac{-V_e}{l}\sin\overline{\phi}_e}_{\text{constant}} \Rightarrow \widehat{e}_\delta(t) = \widehat{e}_\delta(\widehat{t}_1) - (t - \widehat{t}_1)\frac{V_e}{l}\sin\overline{\phi}_e.$$

Recall also that angle $\widehat{e}_\delta$ achieves its critical value $\widehat{e}_{\delta,cr}$ at time $\widehat{t}_2$. Therefore:

$$\widehat{e}_{\delta,cr} = \widehat{e}_\delta(\widehat{t}_1) - (\widehat{t}_2 - \widehat{t}_1)\frac{V_e}{l}\sin\overline{\phi}_e \Rightarrow$$
$$\widehat{t}_2 - \widehat{t}_1 = \frac{l}{V_e\sin\overline{\phi}_e}\left(\widehat{e}_\delta(\widehat{t}_1) - \widehat{e}_{\delta,cr}\right).$$

By substituting the values of $\widehat{t}_1, \widehat{e}_\delta(\widehat{t}_1)$ and $\widehat{e}_{\delta,cr}$ from (25), (26) and (24), respectively, we obtain the value of $\widehat{t}_2$ which is shown in (28).

D. Characterizing the Value of $\widehat{t}_f$:

Combining the values of $\widehat{t}_1, \widehat{t}_2$ along with (23) we can compute the final value of $\widehat{t}_f$ as shown in (29).

$$\widehat{t}_1 = \frac{\overline{\phi}_e - \phi_{e0}}{\overline{\omega}} \tag{27}$$

$$\widehat{t}_2 = \widehat{t}_1 + \frac{l}{V_e \sin \overline{\phi}_e}\left(e_{\delta 0} - \frac{V_e}{l\overline{\omega}}(\cos\phi_{e0} - \cos\left(\overline{\omega}\widehat{t}_1 + \phi_{e0}\right)) - \left(\frac{\pi}{2} - \varepsilon\right) - \frac{V_e}{l\underline{\omega}}\cos\overline{\phi}_e\right) \tag{28}$$

$$\widehat{t}_f = \widehat{t}_2 + \frac{-\overline{\phi}_e}{\underline{\omega}} \tag{29}$$

E. Characterizing the Enlarged Controlled Invariant Set

In the previous subsections, we were able to characterize the maneuver parameters calculated as function of the initial conditions ϕ_{e0} and $e_{\delta 0}$. We now characterize how the distance $\widehat{e}_r$ evolves along the different phases of the maneuver as a function of the initial condition e_{r0}. The controlled invariant set R then constitutes of all the initial conditions $(e_{r0}, e_{\delta 0}, \phi_{e0})$ for which the distance $\widehat{e}_r$ remains strictly positive for the time period $0 \leq t \leq \widehat{t}_f$. For this end, we need to evaluate the dynamics of $\widehat{e}_r$ along the three phases. This can be done by integrating:

$$\dot{\widehat{e}}_r = V_e \cos\widehat{\phi}_e \cos\widehat{e}_\delta - V_p$$

after substituting the corresponding values of $\widehat{\phi}_e$ and $\widehat{e}_\delta$.

1) Phase 1: The decrease in the distance between the evader and the pursuer through this time period can be calculated as:

$$\widehat{e}_r(t) = e_{r0} - V_p t + V_e \alpha_{\overline{\omega}}(0, t, \phi_{e0}, e_{\delta 0}) \tag{30}$$

where:

$$\alpha_\omega(\tau, \tau', a, b) = \int_\tau^{\tau'} \cos\left(\omega t + a\right). \cos\left(b - \frac{V_e}{l\omega}(\cos a - \cos\left(\omega t + a\right))\right) dt. \tag{31}$$

Note that the the term $\int cos(cos\ t)dt$ can not be evaluated in closed-form as it gives rise to the hypergeometric function. Although the previous integration can be computed numerically for given a, b, τ, τ' parameters, for the sake of finding a closed-form description of the safe set, we continue by bounding the previous integration as follows. First, recall that $\cos\theta$ takes values in the set $[-1, 1]$, hence:

$$-1 \leq \cos\left(\omega t + \phi_e\right)\cos\left(e_\delta - \frac{V_e}{l\omega}(\cos\phi_e - \cos\left(\omega t + \phi_e\right))\right) \leq 1.$$

Using this fact, we can bound $\alpha_\omega(\tau, \tau', a, b)$ as:

$$-(\tau' - \tau) \leq \alpha_\omega(\tau, \tau', a, b) \leq \tau' - \tau. \tag{32}$$

Substituting (32) in (30) we conclude that:

$$\widehat{e}_r(t) \geq e_{r0} - (V_p + V_e)t.$$

2) Phase 2: Unlike the previous analysis, we can calculate the exact decrease in the distance $\widehat{e}_r$ during phase 2 as:

$$\dot{\widehat{e}}_r = V_e \cos\overline{\phi}_e \cos\left(\widehat{e}_\delta(\widehat{t}_1) - (t - \widehat{t}_1)\frac{V_e}{l}\sin\overline{\phi}_e\right) - V_p \Rightarrow$$

$$\widehat{e}_r(t) = \widehat{e}_r(\widehat{t}_1) - V_p(t - \widehat{t}_1) + V_e \alpha_2(\widehat{t}_1, t, \overline{\phi}_e, \widehat{e}_\delta(\widehat{t}_1))$$

where:

$$\begin{aligned}\alpha_2(\tau, \tau', a, b) &= \int_\tau^{\tau'} \cos a \cos\left(b - (\tau' - \tau)\frac{V_e}{l}\sin a\right) dt \\ &= \cos a \int_\tau^{\tau'} \cos\left(b - (\tau' - \tau)\frac{V_e}{l}\sin a\right) dt \\ &= -\frac{l\cos a}{V_e \sin a}\sin\left(b - (\tau' - \tau)\frac{V_e}{l}\sin a\right) \\ &= -\frac{l\cot a}{V_e}\sin\left(b - (\tau' - \tau)\frac{V_e}{l}\sin a\right)\end{aligned}$$

from which we conclude that:

$$\begin{aligned}\widehat{e}_r(t) = \widehat{e}_r(\widehat{t}_1) - V_p(t - \widehat{t}_1) \\ - l\cot\overline{\phi}_e \sin\left(\widehat{e}_\delta(\widehat{t}_1) - (t - \widehat{t}_1)\frac{V_e}{l}\sin\overline{\phi}_e\right).\end{aligned}$$

3) Phase 3: Similarly to Phase 1, the decrease in the distance $\widehat{e}_r$ can be calculated as:

$$\begin{aligned}\widehat{e}_r(t) &= \widehat{e}_r(\widehat{t}_2) - V_p(t - \widehat{t}_2) + V_e \alpha_{\underline{\omega}}(\widehat{t}_2, t, \phi_e(\widehat{t}_2), \delta_e(\widehat{t}_2)) \\ &\geq \widehat{e}_r(\widehat{t}_2) - (V_p + V_e)(t - \widehat{t}_2).\end{aligned}$$

Combining all the results together, we conclude that at the end of the proposed maneuver, the distance $\widehat{e}_r(\widehat{t}_f)$ can be bounded as:

$$\begin{aligned}\widehat{e}_r(\widehat{t}_f) \geq e_{r0} - \widehat{t}_f V_e - (\widehat{t}_1 - \widehat{t}_2 + \widehat{t}_f)V_p \\ - l\cot\overline{\phi}_e \sin\left(\widehat{e}_\delta(\widehat{t}_1) - (\widehat{t}_2 - \widehat{t}_1)\frac{V_e}{l}\sin\overline{\phi}_e\right).\end{aligned} \tag{33}$$

We denote the right hand side of the previous inequality as $\widehat{e}_r(x_{e0}, y_{e0}, \theta_{e0}, \phi_{e0})$. Indeed, if by the end of the maneuver the distance $\widehat{e}_r(x_{e0}, y_{e0}, \theta_{e0}, \phi_{e0})$ is strictly positive, then the car would have escaped from the pursuer (pedestrian) and entered the controlled invariant set. The preceding discussion can be summarized in the following result.

Proposition 4.1: Consider an evader (car) modeled by the abstracted dynamics in equations (20) through (22) and a pursuer (pedestrian) modeled by equations (5) through (7). If, at time $t = 0$, the evading car is in the set:

$$R = S \cup \left\{(x_e, y_e, \theta_e, \phi_e) \in \mathbb{R}^2 \times \mathbb{S}^2 \mid \widehat{e}_r(x_e, y_e, \theta_e, \phi_e) > 0\right\}$$

then there is a control strategy for the evader such that for every control strategy of the pursuer no collision occurs. Moreover, the strategy for the evader is given by (19) with $t_1 = \widehat{t}_1, t_2 = \widehat{t}_2, t_f = \widehat{t}_f$ and $\widehat{t}_1, \widehat{t}_2, \widehat{t}_f$ given by (27), (28), and (29), respectively.

It is worth mentioning that the previous result can be extended directly beyond point capture by considering the vehicle dimensions. That is, if h denotes the car length, a sufficient condition for evading the pursuer is that $\widehat{e}_r(x_{e0}, y_{e0}, \theta_{e0}, \phi_{e0})$ is strictly larger than h.

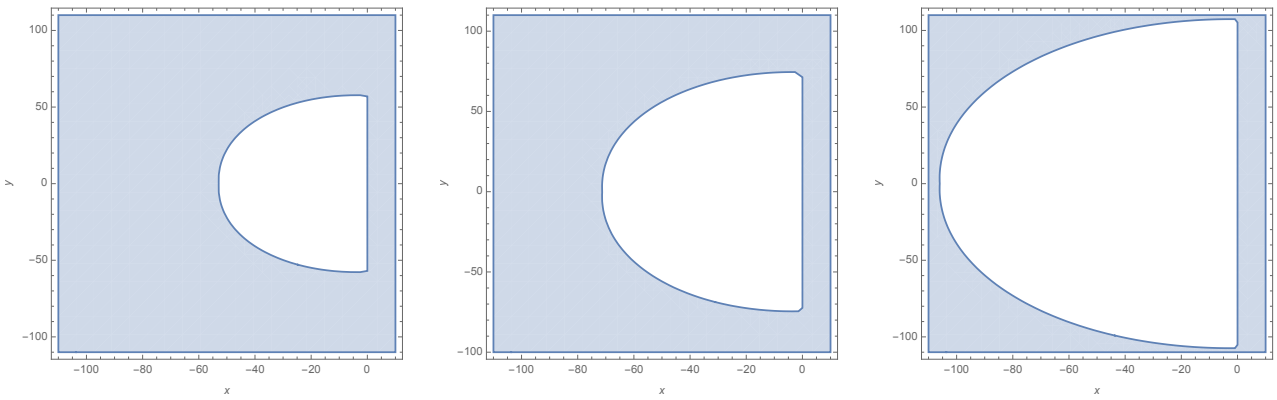

(a) $\overline{\omega} = 0.418879\ rad/s$ (b) $\overline{\omega} = 0.318879\ rad/s$ (c) $\overline{\omega} = 0.218879\ rad/s$

Fig. 2. Effect of changing the upper bound $\overline{\omega}$ on the wheel angular velocity. The controlled invariant set is represented in blue for a pursuer located at the origin, $\theta_e(0) = 0rad$, $\phi_e(0) = 0\ rad$, $l = 4.80\ m$, $\overline{\phi}_e = -\underline{\phi}_e = 0.418879\ rad$, $V_e = 15.646\ m/s$, and $V_p = 1.34\ m/s$.

V. Collision Avoidance For the Original Dynamics

In this section, we strengthen the previous result by considering the original dynamics of the evader (car) described in (1)-(4), or equivalently (17), (18) and (12), instead of the abstracted dynamics. In particular, we show in this section that the analysis carried over the abstracted dynamics leads to a conservative, i.e., under approximation, of the controlled invariant set R. Therefore, by applying the same maneuver—designed for the abstracted dynamics—on the original dynamics, one can always escape from the pursuer. This is captured by the following theorem.

***Theorem** 5.1:* Consider an evader (car) modeled by equations (1) through (4) and a pursuer (pedestrian) modeled by equations (5) through (7). If, at time $t = 0$, the evading car is in the set R defined in Proposition 4.1, then there is a control strategy for the evader such that for every control strategy of the pursuer no collision occurs. Moreover, the strategy for the evader is given by (19) with $t_1 = \widehat{t}_1, t_2 = \widehat{t}_2, t_f = \widehat{t}_f$ and $\widehat{t}_1, \widehat{t}_2, \widehat{t}_f$ given by (27), (28), and (29), respectively.

Proof: First, we recall that the approximate dynamics are obtained from the original dynamics by ignoring the term $\frac{1}{e_r} V_e \sin e_\delta \cos \phi_e$ in (18), i.e.,

$$\dot{e}_\delta = \dot{\widehat{e}}_\delta - \frac{1}{e_r} V_e \sin e_\delta \cos \phi_e.$$

Now it follows from the fact that ϕ_e lies in the range $-\pi/2 < \phi_e < \pi/2$ (recall the assumptions on the model after equation (4)) that $\cos \phi_e$ is always positive. It also follows from the definition of e_r that $1/e_r$ is also positive. Therefore, the sign of the term $\frac{1}{e_r} V_e \sin e_\delta \cos \phi_e$ depends only on $\sin e_\delta$.

Consider the case when e_δ lies in the second quadrant. In this case, $\sin e_\delta$ is positive and hence the term $-\frac{1}{e_r} V_e \sin e_\delta \cos \phi_e$ is negative. This in turn implies that:

$$\dot{e}_\delta \geq \dot{\widehat{e}}_\delta. \tag{34}$$

Now recall that the maneuver (19) is designed to decrease e_δ whenever e_δ starts in the second quadrant until it enters the first quadrant and hence escape from the pursuer. Combining this fact along with (34), which shows that e_δ decreases faster than $\widehat{e}_\delta$, we conclude that e_δ reaches the first quadrant faster than $\widehat{e}_\delta$. That is, by applying the maneuver (19) to the actual evader dynamics, we guarantee that the evader enters the set S faster than the calculated $\widehat{t}_f$ and hence escapes from the pursuer. Similar arguments can be made whenever e_δ lies in the third quadrant. ■

VI. Numerical Results

In this section we numerically illustrate the proposed maneuver. In particular, we show the controlled invariant set for a pursuer located at the origin and for different model parameters. In what follows, we assume that the car is moving with a speed $V_e = 15.6464\ m/s$ (equivalent to the speed limit of 35 mph in US cities), a pedestrian moving with a speed $V_p = 1.34\ m/s$ (average walking speed), car length $l = 4.8\ m/s$ (current average car length), $\overline{\omega}_e = 0.418879\ rad/s$ (equal to spinning the steering wheel with one complete spin per second and a standard steering ratio between the steering wheel and the car wheels of $15:1$).

We start by showing the controlled invariant set, calculated using (33), in Fig. 2 (a) when the car starts with a steering angle $\phi_e(0) = 0$ and orientation $\theta_e(0) = 0$. We can see that when the pursuer is behind the evader (positive x axis) the evader is safe as it can simply drive forward at maximum speed. When the pursuer is in front of the evader, the white area describes all the values of (x_e, y_e) for which the pursuer can force a collision. This region must be avoided by the evader. Next, we study the effect of changing the saturation limits of the wheel angular velocity $\overline{\omega}_e$ (input to the system). Intuitively, as the evader can steer its wheels faster, it can turn away from the pursuer faster and thus also escape faster. This intuition is mirrored in Fig. 2 where we can appreciate how the size of the controlled invariant set (represented in blue) increases as $\overline{\omega}_e$ increases.

Finally, we study the effect of using the abstract dynamics when calculating the controlled invariant set. We split this study into two parts: (i) the effect of abstraction performed when calculating the integral (31) and (ii) the effect of

ignoring the the second term in the $\widehat{e}_\delta$ dynamics (18).

First, we consider the effect of the abstraction performed when calculating the integral (31). Recall that this integral can not be analytically evaluated and hence we relied on coarse upper and lower bounds for the integral. However, we note that such integral can be evaluated numerically for given car parameters. In Fig. 3 we show the difference in the controlled invariant set between the closed-form expression and the numerically computed controlled invariant set. Recall that the numerical integration is not used to determine the maneuver parameters (t_1, t_2 and t_f) but rather to evaluate whether a particular vehicle state (x, y, θ_e, ϕ_e) belongs to the controlled invariant set or not. This in turn affects when the avoidance maneuver needs to be carried over. Fig. 3 shows that an autonomous vehicle located at $y = 0$ and facing a pedestrian can avoid collision provided their distance is greater than 50 meters when using the over-approximated integral. This distance reduces to about 20 meters when using the numerically evaluated integral. These results suggest that, based on the computational power available in the autonomous vehicle, performing numerical integration online (or via the help of pre-computed lookup tables) in the car leads to less conservative estimates of the invariant set and thus of when to initiate an evasive maneuver.

To study the effect of ignoring the the second term in the $\widehat{e}_\delta$ dynamics, we numerically compute the evolution of e_r for both the original dynamics and the abstract dynamics when the proposed evasion maneuver is applied. Fig. 4 shows the evolution of e_r for the two dynamics when the autonomous vehicle starts from $x_e = -25\ m, y_0 = 0\ m, \theta_e = 0\ rad, \phi_e = 0\ rad$. The results shown in Fig. 4 suggests that the maximum difference in the evolution of e_r is around $5\ m$. Comparing this result with the one in Fig. 3 (which shows a difference of $30\ m$), we conclude that the abstraction performed in calculating the integral (31) has a greater effect on the conservativeness of the results compared to the effect of ignoring the second term in the $\widehat{e}_\delta$ dynamics. Repeating the same experiment multiple times using different initial conditions leads to similar results.

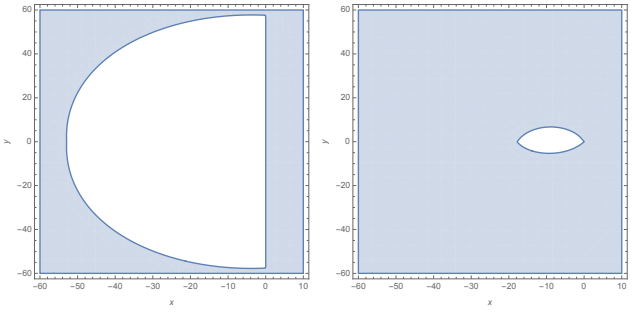

Fig. 3. Effect of over approximating the integral (31): (left) controlled invariant set computed using the closed-form expression (33) and (right) controlled invariant set computed using numerical integration.

VII. Conclusions

In this paper we presented a closed-form expression for a controlled invariant set that leads to a solution of the pedestrian avoidance problem. The straightforward way to obtain a controller from the controlled invariant set is to choose a control input that forces the autonomous car to remain in the invariant set. This strategy typically leads to very aggressive controllers that enable any input when far from the boundary of the controlled invariant set and apply inputs of large magnitude when approaching the boundary. Less aggressive controllers can be obtained by resorting to the recently introduced notion of control barrier function [9], [10]. We are currently investigating how to construct a control barrier function from the controlled invariant set so as to enforce collision avoidance while maximizing passenger comfort.

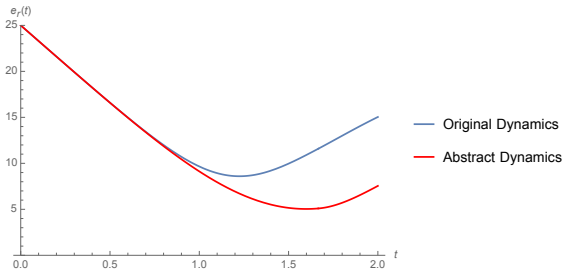

Fig. 4. Evolution of $e_r(t)$, evaluated numerically, after applying the proposed evasive maneuver on the original dynamics (blue) versus the abstract dynamics (red) for the scenario where $x_e(0) = -25\ m, y_e(0) = 0\ m, \theta_e(0) = 0\ rad, \phi_e(0) = 0\ rad, V_e = 15.6464\ m/s, V_p = 1.34112\ m/s$.

References

[1] I. Exarchos, P. Tsiotras, and M. Pachter, "On the suicidal pedestrian differential game," *Dynamic Games and Applications*, vol. 5, no. 3, pp. 297–317, 2015.

[2] R. Isaacs, *Differential Games: A Mathematical Theory with Applications to Warfare and Pursuit, Control and Optimization*. Dover Publications, 1999, unabridged republication. Originally published in 1965 by John Wiley and Sons, Inc., New York.

[3] V. S. Patsko and V. L. Turova, "Homicidal chauffeur game: History and modern studies," in *Advances in Dynamic Games*, ser. Annals of the International Society of Dynamic Games. Boston: Birkauser, 2010, vol. 11, pp. 227–251.

[4] S. Karaman and E. Frazzoli, "Sampling-based algorithms for optimal motion planning," *International Journal of Robotics Research*, vol. 30, no. 7, pp. 846–894, 2011.

[5] J. Ding, J. Sprinkle, C. Tomlin, S. S. Sastry, and J. L. Paunicka, "Reachability calculations for vehicle safety during manned/unmanned vehicle interaction," *AIAA Journal of Guidance, Control and Dynamics*, vol. 35, no. 1, pp. 138–152, 2012.

[6] S. D. Bopardikar, F. Bullo, and J. P. Hespanha, "A cooperative homicidal chauffeur game," *Automatica*, vol. 45, no. 7, pp. 1771–1777, 2009.

[7] I. Exarchos, P. Tsiotras, and M. Pachter, "UAV collision avoidance based on the solution of the suicidal pedestrian differential game," in *AIAA Guidance, Navigation, and Control Conference, San Diego, CA*, 2016.

[8] A. De Luca, G. Oriolo, and C. Samson, "Feedback control of a nonholonomic car-like robot," in *Robot motion planning and control*. Springer, 1998, pp. 171–253.

[9] A. D. Ames, J. W. Grizzle, and P. Tabuada, "Control barrier function based quadratic programs with application to adaptive cruise control," in *Proceedings of the IEEE Conference on Decision and Control (CDC)*, 2014.

[10] X. Xu, P. Tabuada, J. W. Grizzle, and A. D. Ames, "Robustness of control barrier functions for safety critical control," in *Proceedings Analysis and Design of Hybrid Systems (ADHS)*, 2015.